

Regulation under Disturbances with Multiple Harmonics of Unknown Frequency

Alex Esbrook, Xiaobo Tan, and Hassan K. Khalil

Abstract—In this paper, we address the regulation problem for a linear plant driven by a neutrally stable exosystem. It is assumed that the plant is subjected to an exogenous disturbance, and that this signal is formed of known harmonics of a sinusoidal reference signal whose frequency is unknown. Such an exosystem is motivated by the case where the system possesses an input nonlinearity like hysteresis. We propose an adaptive servocompensator requiring estimation of only the primary frequency. Using two-time-scale analysis, we establish the semi-global convergence of the parameter error to an arbitrarily small neighborhood of zero, when the adaptation gain is small enough and when the disturbance is sufficiently small comparing to the reference signal. The proposed control scheme involves far fewer adaptation variables than existing methods, and its performance is verified in both simulation and experiments conducted on a nanopositioning stage.

I. INTRODUCTION

The subject of adaptive regulation theory has seen several developments over the past years. Such work is based on the adaptation of an internal-model based controller to compensate for disturbances injected into the system by a neutrally stable exosystem. However, just what form that internal model controller takes varies greatly from one method to the next. The work reported in [1] and by others proposed parameter-based adaptation of the controller parameters in the internal model transfer function. Work on nonlinear regulation has produced more varied designs such as that proposed by Serrani *et al* [2] where a stable system together with an adaptive state feedback was utilized to generate an internal model controller. In the most recent works, nonlinear internal models have become common. For example, in [3], internal model possesses linear state dynamics but a nonlinear output function. Nikiforov designed an adaptive observer in [4] to estimate and then cancel disturbances generated by a linear exosystem, while Priscoli *et al.* [5] dealt with the design of adaptive observers for nonlinear exosystems.

One feature shared by all the aforementioned methods is that the internal models tend to have many adapted parameters. This allows them to adapt to very diverse exosystems, assuming that the internal model controller is of appropriate order. In several instances of practical importance, the structure of the nonlinearities and disturbances

in the system restricts the set of possible exosystems. For example, consider the setup in [6], where the reference is a sinusoid and disturbances in the system are generated by a nonlinear operator, namely hysteresis. In such a case, while the exosystem is infinite-dimensional, it can be parameterized as a function of only one unknown variable, the primary reference frequency. If we consider a finite dimensional approximation, the exosystem for such a system can be written as

$$\dot{\sigma} = S(w_r, \zeta)\sigma \quad (1)$$

where w_r is the reference frequency, $\zeta \in \mathfrak{R}^n$ is a known constant vector of whole numbers, and the structure of S with respect to w_r and ζ is known. By this structure, we imply that all disturbances have frequencies at multiples of the reference signal's frequency, in particular at $\zeta_i w_r$, $i = 1, \dots, n$. Frequency estimation has been a commonly explored topic in the literature (see [7], [8], [9] and others). However, most often these works are not aimed at regulation, and need to estimate frequencies, amplitudes, and phases of the signals in question in order to cancel them.

In order to deal with systems like those discussed above, we will consider systems comprised of a linear plant $G_p(s)$, represented in the state-space as

$$\begin{aligned} \dot{x} &= Ax + B(u(t) + \alpha(t)) \\ y(t) &= Cx \end{aligned} \quad (2)$$

where $u(t)$ is a control signal, and $\alpha(t)$ is a matched disturbance. The control objective is to regulate the tracking error $e(t) = y_r(t) - y(t)$ to zero, where

$$y_r(t) = R_r \sin(w_r t) \quad (3)$$

is the reference, but the frequency w_r and the amplitude are unknown. The disturbance $\alpha(t)$ is given by

$$\alpha(t) = \sum_{i=1}^n R_{di} (\sin \zeta_i w_r t + \phi_{di}) \quad (4)$$

where the vector $\zeta = [\zeta_1, \zeta_2, \dots, \zeta_n]'$ is known. We will assume that the vector ζ is comprised of increasing whole numbers, such that $\zeta_j > \zeta_k$ if and only if $j > k$. Such a setup is indicative of a linear system with unknown sinusoidal reference and input nonlinearity. Rather than attempting to directly estimate the parameters of the internal model for such a system [6], we will take an indirect adaptive control approach, wherein we use an online adaptive law to estimate the reference frequency, and then use this estimate in an internal model controller. The form of this adaptive law is

The work was supported by the National Science Foundation (CMMI 0824830).

A. Esbrook, X. Tan, and H. K. Khalil are with the Department of Electrical and Computer Engineering, Michigan State University, East Lansing, MI 48824. esbrook@msu.edu (A. E.), xbtan@egr.msu.edu (X. T), khalil@egr.msu.edu (H. K.)

inspired by a formal gradient algorithm, which we modify from its original form to improve stability.

Our analysis and design is based on merging a parameter estimation problem with a linear internal-model controller. A similar approach was taken by Brown and Zhang in [10]. We design our internal model controller in terms of w_r and ζ . We then utilize slow adaptation to separate the estimation of w_r from the dynamics of the plant and time-varying internal model controller. Using the two-time-scale averaging framework of [11], we will show stability of the closed-loop system and practical regulation of the output. For the class of systems in question, this controller is capable of generating the same internal model as the aforementioned adaptive internal model controllers [1]–[5], but requiring far fewer adapted variables.

Another practical advantage the proposed controller has is that it is capable of compensating disturbances generated by the exosystem that are small in a norm sense. While pursuing the work reported in [6], we found that the method used there struggled to adapt the internal model to compensate for smaller harmonics generated by the nonlinearity hysteresis. The problems encountered in that work represent the key motivation for the current work. The proposed method is able to avoid this problem by needing only to estimate a parameter related to the much larger reference trajectory. Simulation results will demonstrate that, with a sufficiently small adaptation gain, arbitrarily small parameter error and regulation error can be achieved. We will also verify our results experimentally on a commercial nanopositioning stage.

The remainder of this paper is organized as follows. In Section II, we present the design of the stabilizing and internal model controllers, as well as the form of the adaptive law. The analysis of the system is presented in three parts. We first stabilize the boundary layer system in Section III-A. Second, in Section III-B we prove the stability of the average system when $\alpha = 0$. Finally, the case where $\alpha \neq 0$ is addressed in Section III-C to address the case where the exosystem has a higher order. We then verify the performance of the method by simulation and experimental results in Section IV. Finally, concluding remarks and future work are presented in Section V.

II. CONTROLLER DESIGN

Based on the internal model principle [12], [13], we design a servocompensator for the system (2)-(4). We define the servocompensator $C(s)$, with state $\eta = [\eta_1, \eta_2, \dots, \eta_{2n}]'$ and input $e(t)$, as

$$\dot{\eta} = \bar{\mathbf{C}}^*(w)\eta + \bar{\mathbf{B}}^*e(t) \quad (5)$$

where

$$\bar{\mathbf{C}}^*(w) = \begin{bmatrix} \mathbf{C}^*(w) & 0 & \dots & 0 \\ 0 & \zeta_1 \mathbf{C}^*(w) & \dots & 0 \\ \vdots & & \ddots & \vdots \\ 0 & \dots & 0 & \zeta_n \mathbf{C}^*(w) \end{bmatrix}, \bar{\mathbf{B}}^* = \begin{bmatrix} k_c \mathbf{B}^* \\ \kappa_1 \mathbf{B}^* \\ \vdots \\ \kappa_n \mathbf{B}^* \end{bmatrix}$$

$$\mathbf{C}^*(w) = \begin{bmatrix} 0 & -w \\ w & 0 \end{bmatrix}, \mathbf{B}^* = \begin{bmatrix} 0 \\ 1 \end{bmatrix}$$

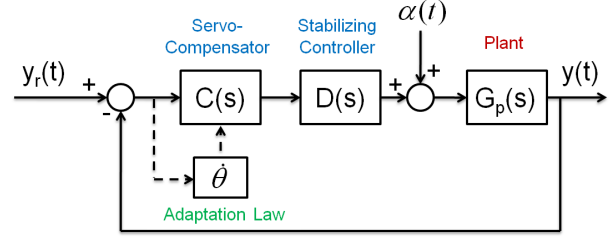


Fig. 1. Block Diagram of the closed-loop system.

and $\kappa = [k_c, \kappa_1, \kappa_2, \dots, \kappa_n]'$, k_c are design parameters assumed to be positive. Based on the work of [12], if the interconnected system (2) - (5) is stable, and $w = w_r$, the tracking error $e(t)$ will go to zero. To stabilize the interconnected system, we design a stabilizing compensator $D(s)$, given in the state-space as

$$\dot{\xi} = A_d \xi + B_d(k_\eta(w)\eta + D_c(w)e(t)) \quad (6)$$

The control signal to the plant (2) is then given by

$$u(t) = C_d \xi + D_d(k_\eta(w)\eta + D_c(w)e(t)) \quad (7)$$

$k_\eta(w)$, $D_c(w)$, and κ will be used to define the numerator of $C(s)$ in order to stabilize the system. Since the reference frequency is unknown, the parameter w will be updated by an adaptation law, the goal of which is to drive the parameter error $\tilde{w} = w - w_r$ to zero. The estimation of w will be governed by the following adaptation law,

$$\dot{w} = -\gamma w^2 e(t) 1/s[\eta_2] \quad (8)$$

where $\gamma > 0$ is the adaptation gain, and η_2 represents the second component of the state vector η for $C(s)$. The form of this adaptation law was originally derived from a formal gradient approach, then modified into that in (8) to improve stability. Throughout the paper, the notation $F(s)[g(t)]$ will denote filtering of the time-domain signal $g(t)$ by the transfer function $F(s)$. Equations (2) to (8) form a complete description of the closed-loop system, represented in the block diagram shown in Fig. 1.

III. SYSTEM ANALYSIS

We will use the two-time-scale averaging framework of [11] to analyze this system. In order to make use of the results of [11], we must define the fast and slow systems, called the boundary-layer system and the average system respectively in the two-time-scale literature. Two-time-scale averaging theory then allows us to analyze the behavior of the two systems *independently*, assuming that the adaptation gain $\gamma \ll 1$ is sufficiently small. In particular, this framework allows us to separate the parameter identification problem from the stabilization and regulation problems.

A. Boundary-Layer (BL) System

The boundary-layer system is defined by combining (2) - (7), and setting $\gamma = 0$ in (8). This fixes the value of w at w_{bl} .

Denoting the state variables of the boundary-layer system as $\chi_{bl} = [\chi'_{bl}, \eta'_{bl}, \zeta'_{bl}]'$, the closed-loop system is then,

$$\begin{aligned} \dot{\chi}_{bl} &= F_{bl}(\chi_{bl}, w_{bl}, t) \\ &= \begin{bmatrix} A - BD_d D_c(w_{bl})C & BD_d k_\eta(w_{bl}) & BC_d \\ -\tilde{\mathbf{B}}^* C & \tilde{\mathbf{C}}^*(w_{bl}) & 0 \\ -B_d D_c(w_{bl})C & B_d k_\eta(w_{bl}) & A_d \end{bmatrix} \chi_{bl} \\ &+ \begin{bmatrix} BD_d D_c(w_{bl})y_r(t) + B\alpha(t) \\ \mathbf{B}^* y_r(t) \\ B_d D_c(w_{bl})y_r(t) \end{bmatrix} \end{aligned} \quad (9)$$

Our first step in the analysis is to show the input-to-state stability (ISS) of the BL system. To achieve this stability, we have the freedom to design both the stabilizing compensator $D(s)$ as well as the numerator of $C(s)$, denoted as $C_n(s)$. We will stabilize the system using frequency domain techniques. First, we design $D(s)$ to stabilize the transfer function

$$H(s) = \frac{D(s)G_p(s)}{1 + D(s)G_p(s)} \quad (10)$$

This stabilizing controller provides a given phase margin at the gain crossover frequency ω_{gc} . Next, we can evaluate the servocompensator transfer function $C(s)$ as

$$C(s) = \frac{C_n(s)}{(s^2 + w_{bl}^2)(s^2 + \zeta_1^2 w_{bl}^2) \cdots (s^2 + \zeta_n^2 w_{bl}^2)} \quad (11)$$

If $k_\eta(w_{bl})$ and $D_c(w_{bl})$ are designed so that

$$C_n(s) = (s^2 + 2\zeta_c w_{bl} s + w_{bl}^2)(s^2 + 2\zeta_c \zeta_1 w_{bl} s + (\zeta_1 w_{bl})^2) \cdots \quad (12)$$

with $\zeta_c \ll 1$, we can approximately cancel the effect of $C(s)$ on the stability of the closed-loop system, assuming that w_{bl} is far enough away from ω_{gc} . This is a crucial step in being able to counteract the effect of the servocompensator on the stability of the system. Otherwise, it is a very difficult task to stabilize the system over a wide range of possible reference frequencies. For the framework of [11] to apply, it is also required that the solutions of (9) are asymptotically periodic (or almost periodic). In system considered herein, this requirement is easily satisfied since (9) represents an exponentially stable linear system driven by a $2\pi/w_r \triangleq T$ -periodic signals $y_r(t)$ and $\alpha(t)$. It is important to note that if $w_{bl} = w_r$, the tracking error $e(t)$ will be zero in the steady state.

B. Controller & Average System When $\alpha = 0$

We now will analyze the average of (8), defined by the evolution of the average of w , w_{av} , evaluated along the steady-state solutions of the boundary layer system $\chi_{bl}(w)$. We also define the average estimation error, $\tilde{w}_{av} = w_{av} - w_r$. For the remainder of this paper, we will simplify the presentation by writing $G(s) = D(s)G_p(s)$. The average system is defined by

$$\begin{aligned} \dot{w}_{av} &= F_{av}(\chi_{bl}(w_{av}), w_{av}, \vartheta, e) \\ &= -\frac{\gamma}{T} \int_0^T w_{av}^2 e(t) \frac{1}{s} [\eta_2] dt \end{aligned} \quad (13)$$

We split our analysis of the above system into two parts. First, we will deal with the case where $\alpha(t) = 0$, in order to present our analysis more clearly. Then, in Section III-C, we will address the case where $\alpha(t) \neq 0$.

In order to evaluate the integral in (13), we will formulate $F_{av}(\chi_{bl}(w_{av}), w_{av}, \vartheta, e)$ as a function of only the adaptation variable w_{av} and reference trajectory y_r . Proceeding under the assumption that $\alpha(t) = 0$, we can evaluate the controller transfer function as

$$C(s) = \frac{C_n(s)}{s^2 + w_{av}^2} \quad (14)$$

where $C_n(s) = s^2 + 2\zeta_c w_{av} s + w_{av}^2$. Letting $G(s) = G_n(s)/G_d(s)$, we can now evaluate the sensitivity transfer function $S(s)$ as

$$S(s) = \frac{G_d(s)(s^2 + w_{av}^2)}{G_d(s)(s^2 + w_{av}^2) + C_n(s)G_n(s)} \quad (15)$$

This allows us to represent the error $e(t)$ as

$$e(t) = S(s)[y_r(t)] \quad (16)$$

We can arrive at a similar expression for the term $G_f(s)[\eta_2]$. Defining $\eta_2(s)$ as the transfer function from $e(t)$ to $\eta_2(t)$, we arrive at an expression for η_2 ,

$$\begin{aligned} \eta_2(t) &= \eta_2(s)[e(t)] = \frac{sk_c}{s^2 + w_{av}^2} [e(t)] \\ &= \frac{sk_c G_d(s)}{G_d(s)(s^2 + w_{av}^2) + C_n(s)G_n(s)} [y_r(t)] \end{aligned} \quad (17)$$

Using (16) and (17), all the terms inside the integral in (13) are now dependent only on the adaptation parameter w_{av} and reference trajectory y_r . It is well known that given the form of y_r in (3), at steady state the terms $e(t) \triangleq A(s)[y_r(t)]$ and $1/s[\eta_2(t)] \triangleq B(s)[y_r(t)]$ will evaluate to terms of the form $R \sin(w_r t + \phi)$, where R and ϕ depend on the magnitudes and phases of $A(s)$ and $B(s)$. Using this, we can now evaluate the integral in (13) as

$$F_{av}(\cdot) = -\frac{\gamma w_{av}^2 |A(jw_r)| |B(jw_r)| R_r^2}{2} \cos(\phi_A - \phi_B) \quad (18)$$

where $\phi_A = \angle A(jw_r)$, and $\phi_B = \angle B(jw_r)$. It is clear that the properties of the average system depend heavily on the terms $|A(jw_r)|$, $|B(jw_r)|$, ϕ_A , and ϕ_B . Note that $A(s) = S(s)$, and $B(s) = 1/s \eta_2(s) S(s)$. To simplify the coming expressions, we will use the shorthand notation,

$$S_d(s) = G_d(s)(s^2 + w_{av}^2) + C_n(s)G_n(s) \quad (19)$$

First, we evaluate the magnitude of $A(jw_r)$ and $B(jw_r)$ as

$$|A(jw_r)| = \frac{|G_d(jw_r)| |w_{av} + w_r| |w_{av} - w_r|}{|S_d(jw_r)|} \quad (20)$$

$$|B(jw_r)| = \frac{k_c |G_d(jw_r)|}{|S_d(jw_r)|} \quad (21)$$

and the phases as

$$\phi_A = \angle G_d(jw_r) + \frac{\pi}{2} \text{sgn}(w_{av} - w_r) - \frac{\pi}{2} - \angle S_d(jw_r) \quad (22)$$

$$\phi_B = \angle G_d(jw_r) - \angle S_d(jw_r) \quad (23)$$

where $\text{sgn}(a)$ represents the sign of a . First, we note that the term $|w_{av} - w_r|$ in (20) is equal to $|\tilde{w}_{av}|$. Second, we subtract (22) from (23) to arrive at the argument of the cosine term in (18),

$$\phi_A - \phi_B = \frac{\pi}{2} \text{sgn}(\tilde{w}_{av}) - \frac{\pi}{2} \quad (24)$$

which implies that

$$\cos(\phi_A - \phi_B) = \cos\left(\frac{\pi}{2} \text{sgn}(\tilde{w}_{av}) - \frac{\pi}{2}\right) = \text{sgn}(\tilde{w}_{av}) \quad (25)$$

We can write (13) as

$$\dot{w}_{av} = - \frac{w_{av}^2 \gamma |G_d(jw_r)| |w_{av} + w_r| |B(jw_r)| R_r^2}{2 |S_d(jw_r)|} \tilde{w}_{av} \quad (26)$$

$$\triangleq -M(w_{av}, w_r) \tilde{w}_{av} \quad (27)$$

where we have used $|w_{av} - w_r| \text{sgn}(\tilde{w}_{av}) = \tilde{w}_{av}$. We can now use (26) to show asymptotic stability of the equilibrium point $\tilde{w}_{av} = 0$. From (19), we note that if the adaptation parameter w and reference frequency is bounded above and below, we can guarantee that $|S_d(jw_r)|$ is finite and nonzero for all w_r and w , where the nonzero property follows from the stability of the boundary-layer system. This implies that $M(w_{av}, w_r)$ is bounded above and below by finite constants $k_h > 0$ and $k_l > 0$ respectively. Next, define the Lyapunov function candidate $V(t) = \tilde{w}_{av}^2/2$, whose time derivative is

$$\begin{aligned} \dot{V} &= \tilde{w}_{av} \dot{w}_{av} = -M(w_{av}, w_r) \tilde{w}_{av}^2 \\ &\leq -k_l V \end{aligned} \quad (28)$$

since $\dot{\tilde{w}}_{av} = \dot{w}_{av}$. Thus, we can conclude exponential stability from the Lyapunov Theorem [14]. Using this result together with the results of Section III-A, the framework of [11] ensures that, for any $\delta > 0$, there exists a pair of class $\mathcal{H}\mathcal{L}$ functions β_s and β_f such that, when the adaptation gain is sufficiently small, the solutions of the complete system (2) to (8) obey the ultimate bounds

$$\begin{aligned} |\tilde{w}(t)| &\leq \beta_s(|\tilde{w}(0)|, t) + \delta \\ |e(t)| &\leq \beta_f(|e(0), \tilde{w}(0)|, t) + \delta \end{aligned} \quad (29)$$

C. Controller & Average System When $\alpha \neq 0$

We now consider the case where $\alpha(t) \neq 0$. The servo-compensator is once again given in the form of (5). The adaptation law will be unchanged from the form in (8). Since the proof requires us to maximize some terms, we introduce the following assumption to establish a bound on w_{av} by bounding w .

Assumption 1: There exists a w_h such that for any ω_h , if the frequency estimate w is constrained to be less than w_h , then w_{av} is less than ω_h .

Theorem 1: Let w and w_r be less than w_h . Let R_r be greater than a known constant c . Consider the system (2) - (8), depicted in Fig. 1. Then, for every δ , there exists a $\gamma_2 > 0$ such that if $\gamma \in (0, \gamma_2)$, the average system is semi-globally exponentially stable, and the trajectories of (2) - (8) satisfy the ultimate bounds

$$\begin{aligned} |\tilde{w}(t)| &\leq \beta_s(|\tilde{w}(0)|, t) + \delta \\ |e(t)| &\leq \beta_f(|e(0), \tilde{w}(0)|, t) + \delta \end{aligned}$$

Proof: The proof follows the same steps as did the analysis for the case where $\alpha = 0$. After showing stability of the boundary-layer system, the first step in the proof is to expand the terms $e(t)$ and $1/s[\eta_2(t)]$ so that they are dependent on only the adaptation parameter, disturbance $\alpha(t)$, and reference trajectory $y_r(t)$. Next, the resulting integral is evaluated, which results in a series of terms related to the transfer functions of the system. By evaluating the magnitudes and phases of these transfer functions, it is possible to prove that the average system possesses a semi-global exponentially stable equilibrium point at $\tilde{w}_{av} = 0$, when the reference amplitude R_r is large enough. The complete details of this proof are omitted for space concerns, but will be available in an upcoming journal paper extending this work. ■

IV. SIMULATION & EXPERIMENTAL RESULTS

A. Simulation Results

We will now demonstrate that the controller is capable of achieving near-zero tracking and parameter error in simulation. Our simulations will be conducted on a 4th order plant designed to model the dynamics of a commercial nanopositioner (Nano-OP65 with Nano-Drive controller, Mad City Labs Inc). The reference trajectory is chosen as $20 \sin(2\pi 200t)$. Motivated by disturbances like (4), the plant is also subjected to a matched disturbance of $3 \sin(2\pi 400t)$. Accordingly, the internal model controller (5) is designed with $\zeta = 2$ to compensate the reference and disturbance. The notch filter parameter ζ_c in (12) was set to .2, and stability over the frequency range of interest is achieved through the use of a stabilizing controller

$$D(s) = \frac{2.083 \times 10^7}{s^2 + 4900s + 1.225 \times 10^7} \quad (30)$$

Simulation results are presented in Fig. 2 and Fig. 3. The results when $w(0) = 2\pi 120$ & $w(0) = 2\pi 280$ are plotted in Fig. 2. With $\gamma = .05$, the parameter error in both cases converged to the order of 10^{-10} . Tracking error was on the order of 10^{-9} after 3 seconds. The fact that the controller is able to drive the parameter and tracking errors to very near zero seems to imply that the ultimate boundedness result acquired through the two-time-scale framework is conservative.

B. Experimental Results

Our experiments are conducted on a commercial nanopositioner (Nano OP-65, Mad City Labs). This nanopositioner has a travel range of $65 \mu\text{m}$. In accordance with the results of [15] and [16], we utilize a feedforward hysteresis inversion to guarantee that the system will possess a stable periodic solution. The stabilizing controller (30) was used to stabilize the feedback connection. Since the reference trajectories required a bias, a low gain proportional-integral controller was added to the system in parallel with the servocompensator.

There are two properties of the controller that we will verify with these experiments. The first property is that our adaptive controller can recover the performance of a nominal

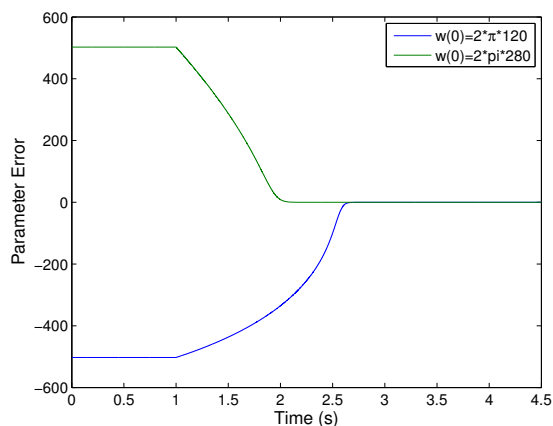


Fig. 2. Parameter error \tilde{w} in 200 Hz simulation. Two different initial conditions are plotted.

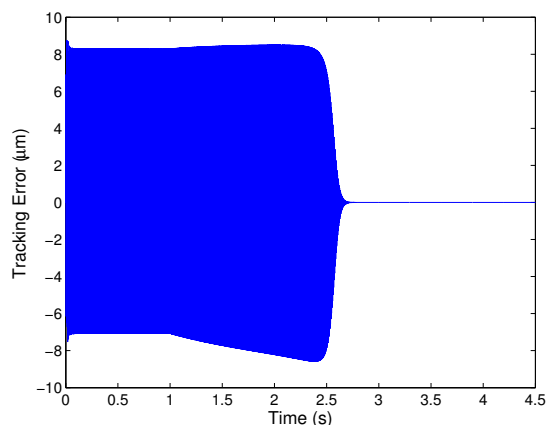


Fig. 3. Tracking error $e(t)$ in 200 Hz simulation. Initial condition is 120 Hz.

controller where the parameters are known. Second, we verify that the controller responds to changes in the reference signals. Both properties should be satisfied by any adaptive internal model controller. We will compare the performance of our various methods via the mean tracking error, computed by taking the mean of $|e(t)|$ over one period of the reference.

Recovery of nominal performance was done with two controller types. First, we use a second-order internal model controller, designed to compensate for the sinusoidal reference signal. Second, we utilize a sixth-order controller, with $\zeta = [2, 3]$. This controller is capable of compensating for the primary reference as well as the first two harmonics of the reference generated by the hysteresis nonlinearity of the piezoelectric. Experiments are conducted with inputs at 5, 25, 50, and 100 Hz. Due to issues with the experimental platform, the amplitude of the reference was changed from 40 μm peak-to-peak at 5 Hz and 25 Hz to 20 μm peak-to-peak at 50 Hz and 100 Hz. The adaptation gain γ was chosen as 0.001 for each frequency.

Fig. 4 and Fig. 5 show the results of this experiment. In both cases, the adaptive controller does very well at

TABLE I
TRACKING ERRORS IN PERCENTAGE OF REFERENCE AMPLITUDE FOR ADAPTED AND NOMINAL SYSTEMS UNDER VARYING INPUTS.

Reference	Second-Order		Sixth-Order	
	Adapted	Nominal	Adapted	Nominal
5Hz	0.4935	0.3715	0.0905	0.097
25Hz	0.5425	0.543	0.216	0.231
50Hz	1.119	1.01	0.302	0.318
100Hz	1.131	1.054	0.535	0.563

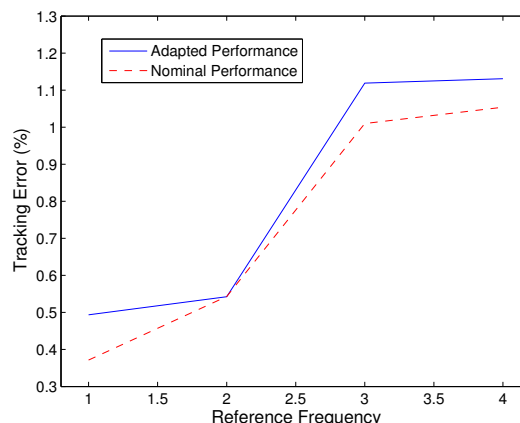


Fig. 4. Tracking error in percentage for adapted and nominal controller, with the second-order internal model.

recovering the nominal controller's performance. It is worth noting however that the sixth-order controller does a better and more consistent job at recovering the performance than the second-order controller. Since the sixth-order controller is able to greatly reduce the tracking error as compared to the second-order controller, the parameter estimation error stays closer to zero over time, which allows the system to behave much closer to the nominal system. A sample of the tracking error for this signal is also presented in Fig. 6.

Next, we examine the controller's performance when the reference signal is changing. The internal model controller

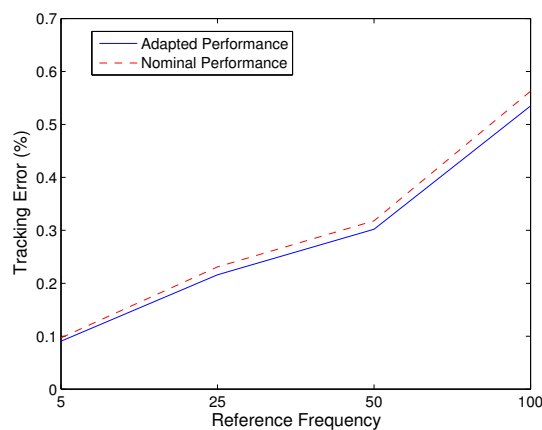


Fig. 5. Tracking error in percentage for adapted and nominal controller, with the sixth-order internal model.

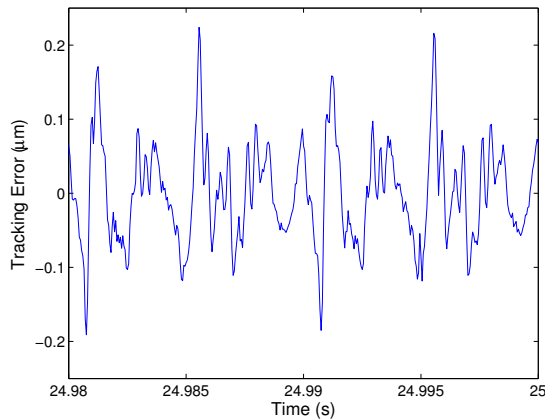


Fig. 6. Tracking error for 100 Hz reference signal with the sixth-order controller.

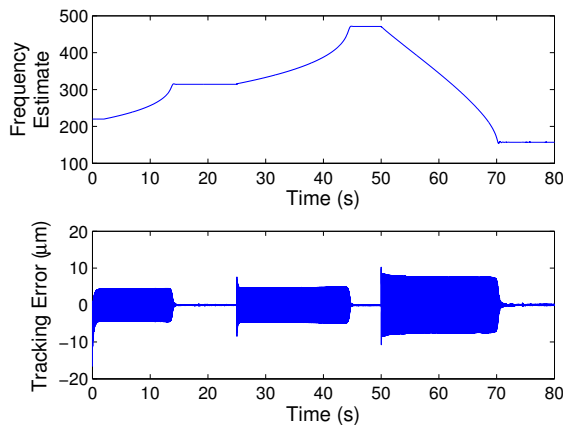


Fig. 7. Frequency Estimate ω and tracking error for a changing reference signal.

used for this experiment was sixth order. Initially, the reference signal was $10\sin(2\pi 50) + 20 \mu\text{m}$. At 25 s, the signal changed to $10\sin(2\pi 75) + 20 \mu\text{m}$, and at 50 s changed to $20\sin(2\pi 25) + 20 \mu\text{m}$. The adaptation gain γ was increased to 0.003 to improve convergence speed. Fig. 7 shows the evolution of the parameter estimate under the changing reference signal. Note that the tracking error, also shown in Fig. 7 is high until the frequency estimate gets very close to the actual value. Once the parameter converges, the tracking error rapidly shrinks to its steady state value.

V. CONCLUDING REMARKS

We have presented the design and analysis of a novel adaptive servocompensator. The method is capable of compensating small signals, like those resulting from hysteresis. In addition, it requires fewer adapted states to compensate for the exosystem considered here than other adaptive regulators. We have also shown through analysis and testing that the estimation error is capable of converging to an arbitrarily small value over a semi-global range. Tracking error performance is comparable to other state-of-the-art methods used

in nanopositioning control.

Strengthening our analytical results will be pursued in our future work. We will seek to generalize the adaptation law and analysis, by considering a wider range of possible disturbances and reference trajectories, such as disturbances where ζ is not made of whole numbers. In addition, we plan on considering reference trajectories consisting of multiple sinusoids or parameterized like the disturbance α , where there is one unknown frequency, and the reference trajectory can be written as a sum of sinusoids with frequencies at known multiples of the unknown frequency. An example of such a reference signal is a sawtooth wave, commonly used in nanopositioning applications.

REFERENCES

- [1] H. Elliott and G. C. Goodwin, "Adaptive implementation of the internal model principle," in *Proceedings of the 23rd IEEE Conference on Decision and Control*, 1984, pp. 1292 – 1297.
- [2] A. Serrani, A. Isidori, and L. Marconi, "Semiglobal nonlinear output regulation with adaptive internal model," *IEEE Transactions on Automatic Control*, vol. 46, no. 8, pp. 1178–1194, 2001.
- [3] Z. Chen and J. Huang, "Global robust servomechanism problem of lower triangular systems in the general case," *Systems & Control Letters*, vol. 52, no. 3, pp. 209–220, 2004.
- [4] V. Nikiforov, "Adaptive nonlinear tracking with complete compensation of unknown disturbances," *European Journal of Control*, vol. 4, pp. 132–139, 1998.
- [5] F. D. Prisco, L. Marconi, and A. Isidori, "Adaptive observers as nonlinear internal models," *Systems & Control Letters*, vol. 55, no. 8, pp. 640–649, 2006.
- [6] A. Esbrook, X. Tan, and H. Khalil, "A robust adaptive servocompensator for nanopositioning control," in *49th IEEE Conference on Decision and Control*, 2010, pp. 3688 –3693.
- [7] M. Mojiri and A. R. Bakhshai, "An adaptive notch filter for frequency estimation of a periodic signal," *IEEE Transactions on Automatic Control*, vol. 49, no. 2, pp. 314–318, 2004.
- [8] M. Bodson and S. C. Douglas, "Adaptive algorithms for the rejection of sinusoidal disturbances with unknown frequency," *Automatica*, vol. 33, no. 12, pp. 2213–2221, 1997.
- [9] X. Xia, "Global frequency estimation using adaptive identifiers," *IEEE Transactions on Automatic Control*, vol. 47, no. 7, pp. 1188–1193, 2002.
- [10] L. J. Brown and Q. Zhang, "Periodic disturbance cancellation with uncertain frequency," *Automatica*, vol. 40, no. 4, pp. 631 – 637, 2004.
- [11] A. R. Teel, L. Moreau, and D. Nesić, "A unified framework for input-to-state stability in systems with two time scales," *IEEE Transactions on Automatic Control*, vol. 48, no. 9, pp. 1526–1544, 2003.
- [12] E. J. Davison, "The robust control of a servomechanism problem for linear time-invariant multivariable systems," *IEEE Transactions on Automatic Control*, vol. 21, pp. 25–34, 1976.
- [13] B. Francis and W. Wonham, "The internal model principle for linear multivariable regulators," *Applied Mathematics and Optimization*, vol. 2, pp. 170–194, 1975.
- [14] H. K. Khalil, *Nonlinear Systems*, 3rd ed. Upper Saddle River, NJ: Prentice Hall, 2002.
- [15] A. Esbrook, M. Guibord, X. Tan, and H. K. Khalil, "Control of systems with hysteresis via servocompensation and its application to nanopositioning," in *Proceedings of the 2010 American Control Conference*, 2010, pp. 6531–6536.
- [16] X. Tan and H. K. Khalil, "Two-time-scale averaging of systems involving operators and its application to adaptive control of hysteretic systems," in *Proceedings of the 2009 American Control Conference*, 2009, pp. 4476–4481.